Journal of Biomedical Optics

BiomedicalOptics.SPIEDigitalLibrary.org

Geometrical and topological analysis of *in vivo* confocal microscopy images reveals dynamic maturation of epidermal structures during the first years of life

Jalil Bensaci
Zhao Yang Chen
M. Catherine Mack
Martial Guillaud
Georgios N. Stamatas

SPIE.

Geometrical and topological analysis of *in vivo* confocal microscopy images reveals dynamic maturation of epidermal structures during the first years of life

Jalil Bensaci,[a,*] Zhao Yang Chen,[b] M. Catherine Mack,[c] Martial Guillaud,[b] and Georgios N. Stamatas[a]
[a]Johnson & Johnson Santé Beauté France, 1 rue Camille Desmoulins, Issy-les-Moulineaux 92130, France
[b]British Columbia Cancer Agency, 675 West 10th Avenue, Vancouver, British Columbia V5Z 1L3, Canada
[c]Johnson and Johnson Consumer Companies Inc., 199 Grandview Road, Skillman, New Jersey 08558, United States

Abstract. Reflectance confocal microscopy is successfully used in infant skin research. Infant skin structure, function, and composition are undergoing a maturation process. We aimed to uncover how the epidermal architecture and cellular topology change with time. Images were collected from three age groups of healthy infants between one and four years of age and adults. Cell centers were manually identified on the images at the stratum granulosum (SG) and stratum spinosum (SS) levels. Voronoi diagrams were used to calculate geometrical and topological parameters. Infant cell density is higher than that of adults and decreases with age. Projected cell area, cell perimeter, and average distance to the nearest neighbors increase with age but do so distinctly between the two layers. Structural entropy is different between the two strata, but remains constant with time. For all ages and layers, the distribution of the number of nearest neighbors is typical of a cooperator network architecture. The topological analysis provides evidence of the maturation process in infant skin. The differences between infant and adult are more pronounced in the SG than SS, while cell cooperation is evident in all cases of healthy skin examined. [DOI: 10.1117/1.JBO.20.9.095004]

Keywords: confocal; topology; entropy; nearest neighbors; infant; skin maturation.

Paper 150400LR received Jun. 12, 2015; accepted for publication Jul. 31, 2015; published online Sep. 11, 2015.

1 Introduction

For a long time, skin research has been performed using invasive methods such as biopsies to collect the necessary samples. Obvious drawbacks of such sampling processes are the risks of interference from even mild inflammation due to the procedure and potential contamination of the sample. Ideally, observations should be done *in vivo*. To address these concerns, several methods have been developed during the last decades, allowing skin observation in a noninvasive way. One of the most informative is *in vivo* reflectance confocal microscopy (RCM), which provides real-time optical transversal sections[1] of the skin area of interest, giving diagnostic information that, in some cases, parallels that of histology and has been recently summarized in these reviews.[2,3] The transversal sections can be acquired at sequential depths with an axial resolution of 3 to 5 μm and arranged in image stacks that document the three-dimensional skin architecture.[4]

In most cases, analysis of the image stacks or individual optical slices is done manually. The results are generally qualitative, providing a description of the tissue sample.[4] In order to obtain more quantitative results,[5,6] the manual analysis becomes even more intensive and is highly time consuming. Paradoxically, despite the amount of information that quantitative analysis can provide, few efforts have been invested so far in developing computational methods to extract it automatically.[7]

One application where *in vivo* RCM has been indispensable is the case of investigations of infant skin, where biopsy is not an ethical option. Baby skin is often considered as a cosmetic aspiration. In reality, it is undergoing a maturation process that takes place during the first years of life,[8,9] characterized by a developing barrier function, which makes it prone to irritations.[10,11] Moreover, differences in structural elements, such as cell size and thickness of layers, may explain the functional differences between infant and adult skin. Such structural differences have been documented noninvasively using *in vivo* RCM.[12]

A deeper understanding of the organization of cell arrangement in space can come from graph theory and concepts like the Voronoi diagram and Delaunay triangulation.[13] Quantitative statistical parameters can then be calculated to characterize the topology of epithelial tissues. Such analysis has been successfully used for the segmentation of epithelial cancers from healthy tissue in digitized histological images[14] and epithelial organizations across different species and kingdoms of life.[15] Another useful parameter is the average number of Delauney nearest neighbors. It has been shown that in many complex cellular structures, cells are most likely to have six neighbors,[16,17] while in other organization types, they might have four or even nine (tumors, for instance).

In this study, we attempt to quantitatively characterize differences in epidermal structures between infant and adult skin

*Address all correspondence to: Jalil Bensaci, E-mail: jbensaci@its.jnj.com

as documented in *in vivo* RCM images by applying principles of geometrical and topological analysis. To our knowledge, this is the first time that this kind of analysis has been performed on RCM images. We then proceed to explore how these parameters may be different between the stratum spinosum (SS) and the stratum granulosum (SG), and how they evolve during the first four years of life.

2 Methods

In vivo RCM image stacks were collected using the Vivascope 1500 instrument (Lucid, Inc., Rochester, New York). The optical resolution is <1.25 μm in the horizontal axis and <5 μm in the vertical one. Imaging started at the top of the SC and progressed down to the top layers of the dermis. The instrument was equipped with a 785 nm laser (power <25 mW at the tissue surface) and produced an optical section every 3.125 μm of increasing depth. The image resolution is 1000×1000 pixels and the viewable section of each individual image is 500×500 μm^2.

Confocal image stacks were collected from the upper inner side of the arms of a cohort of 18 healthy Caucasian infants of ages 14 to 48 months and 10 adults. Subjects were instructed not to apply any skin-care products the morning of the study visit. Inclusion criteria required that the subjects were generally in good health, with no history of skin disorders, and were not using oral or topical steroidal medications. The study was conducted following the approval of an independent institutional review board and in accordance with the Declaration of Helsinki principles. Written informed consent was collected from the adult participants and from the mothers of the children participants. Study participants were divided into four groups: infants aged 12 to 24 months, 24 to 36 months, 36 to 48 months, and adults. In order to get the best possible images, the infants were kept comfortably in their mother's arms so that they would be as relaxed as possible and have limited movements during the measurements. However, many times small motions could not be avoided, which resulted in blurred and unusable images that were excluded from the analysis. Representative optical sections of SG and SS were manually selected based on the qualitative morphology of the cells.[4] At least 10 images were used for each age group and layer (Table 1).

Image analysis was performed according to the following steps:

1. Open image.
2. Define a region of interest (ROI) that includes clearly observable networks of adjacent cells.
3. Identify cell centers (centroids) in the ROI: This step automatically triggers the detection of edges with the Voronoi diagram and the Delaunay triangulation. Mainly, the space was partitioned by edges that were equidistant from the nearest centroids resulting in the Voronoi diagram.[13] In this way, a Voronoi cell comprises all the points around a centroid that are closer to this specific centroid than any other one in the ROI. The related Delaunay triangulation graph is obtained by drawing lines connecting all centroids that have a common Voronoi edge.[18] In our case, the Voronoi polygons represent the cell boundaries and the centroids or nodes in the Delaunay graph represent the cell nuclei. For each polygon, the number of sides corresponds to the number of Delaunay neighbors. Two nuclei are linked (by a Delaunay graph vertex) if they share the same edge. This network of polygons represents the spatial organization of the cells in the selected ROI. In our case, this spatial partition represents the epithelial network of the ROI and allows the calculation of topological and geometrical parameters.
4. Calculate geo-topological parameters.
5. Save parameter data file.

Table 1 Number of images analyzed per age group and epidermal layer.

	Age			
Epidermal layer	12 to 24 months	24 to 36 months	36 to 48 months	Adult
Stratum granulosum	10	17	18	10
Stratum spinosum	15	12	12	12

A JAVA program was developed to compute the Voronoi diagram and its dual Delaunay triangulation graph[19] on each selected ROI (Fig. 1), in order to determine several geometrical and topological parameters: cell density, cell area and perimeter, average distance of the polygon center to the nearest neighbor, structural entropy, and mean number of Delaunay neighbors per cell.

The two-dimensional structural entropy was calculated as follows:[20]

$$\text{Entropy} = \log(N) - \sum \frac{H}{\log(1/H)},$$

where $H = Ai/(\text{ROI area})$, Ai is the area of the i'th Voronoi polygon, and N is the total number of centroids or polygons in the ROI.

Data in the figures are presented as mean $\pm$ one standard deviation. Analysis of variance followed by a post hoc analysis (Tukey's test) were performed for group comparison. Statistical significance was accepted at the level of $\alpha = 0.05$.

Each individual gave written, informed consent. The study was performed following approval from the Allendale investigational review board (Old Lyme, Connecticut).

3 Results

With the exception of structural entropy, the values of all tested parameters follow a gradual change that is significant only in SG, from the youngest group to the adults, as the result of the ongoing structural maturation process (Fig. 2).

In both layers, the average cell density decreases with age (by 40.1% in SG and 8.7% in the SS from the 12- to 24-month group to the adult group), shown in Fig. 2(a), reflecting the increase in the cell projected area.[5] Accordingly, there is an increase in the values of the other geometrical parameters in both layers, from the youngest group to the adult group. The change is more pronounced in SG [Figs. 2(b)–2(d)]: The polygon area increases by 83%, the polygon perimeter by 38%, and the distance to the nearest neighbor by 36%. Structural entropy remains stable

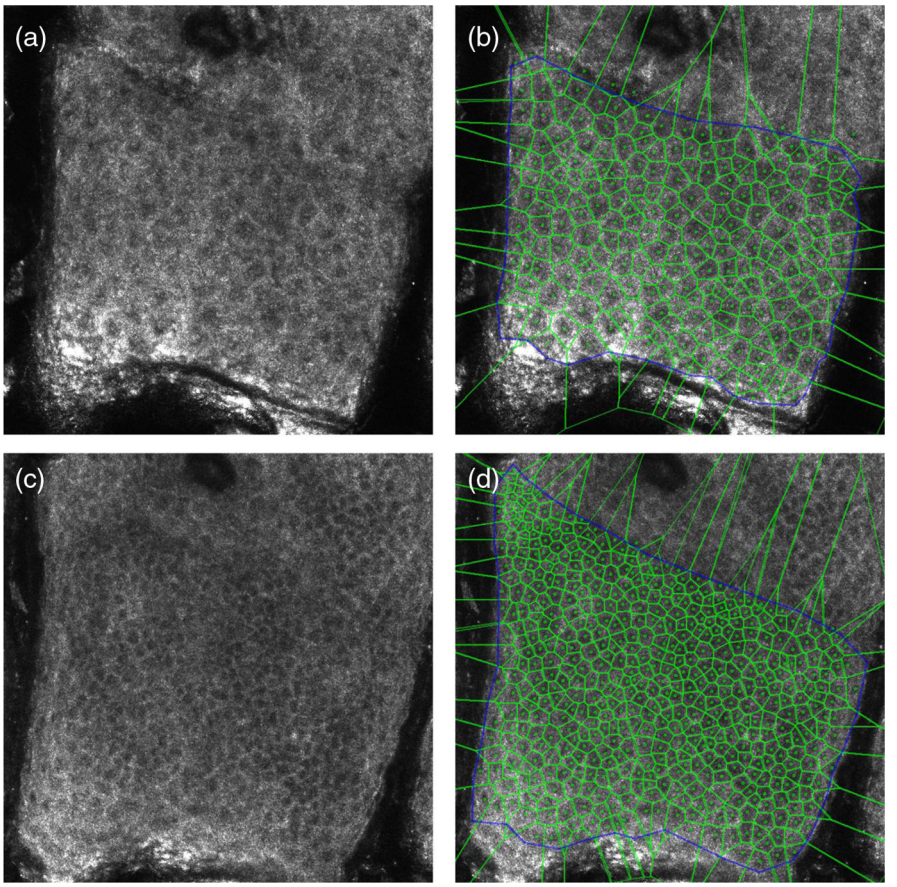

Fig. 1 Examples of reflectance confocal microscopy optical sections at the [(a) and (b)] stratum granulosum (SG) and [(c) and (d)] stratum spinosum (SS). The designated regions of interest are prescribed in blue and the Voronoi diagrams in green [(b) and (d)]. The centroids representing cell centers are marked.

with age in both strata, showing no significant statistical difference between groups of the same stratum [Fig. 2(e)].

Between SS and SG, the values of all tested parameters and for all age groups show statistically significant differences. The cell density is higher in SS than in SG [Fig. 2(a)] by an average of 60%. All the other parameters have a higher value in SG, which is more evident in the adult group. The polygon area shows the most pronounced difference with an SG value 250% higher compared to that of SS; the polygon perimeter value is 88% larger, and the distance to the nearest neighbor is 89% larger.

The number of nearest neighbors for each cell ranges between three and nine, with a mean of six neighbors per cell (Fig. 3). The skewness of the nearest-neighbor distribution is positive for all the groups and skin layers. This departure from normal distribution (the distribution shape is asymmetrically shifted to the right of the mode) indicates that the cells are arranged in a nonrandom fashion. The nearest-neighbors probability distribution qualitatively resembles the organization of cells arising from a cooperators model, with the number of nearest neighbors ranging from three to eight with a maximum at six.[15] This is different from the defector model, typically representing epithelial cancers where the cells tend to adopt a cheating or defective behavior as opposed to cooperation. In a defector model, the cells replicate and differentiate in an uncontrolled way, resulting in a probability distribution more shifted toward higher values, including a small but measurable number of cells having 10 nearest neighbors.

4 Discussion

Studying the network organization of cells using geo-topological parameters allows the researcher to quantitatively define the structural patterns of the tissue and follow their evolution in time. In this work, we applied this analysis on RCM images of human epidermis acquired noninvasively *in vivo*.

We first compared the structure and cell organization between two layers of the viable epidermis, the SG and the SS. Cells are typically larger in the SG compared to SS with higher cell area and larger perimeter. This geometry explains the higher cell density and the shorter nearest-neighbor distance between the centroids in the SS compared with SG. Interestingly, structural entropy values remain statistically similar in each layer, indicating that this parameter is preserved with time despite the maturation process in both spinous and granular layers.

We then turned our attention to dynamic changes of these parameters. Infant skin is known to undergo a continuous development process during the early years of life.[5,8,9] Differences between infant and adult skin functions can be at least partially explained by the difference in their architectural structures. Analysis of geo-topological parameters confirmed the dynamic nature of epidermal structures during this maturation period and provided significant insights about these architectural differences. The average cell area and perimeter increase during the first years of life toward adult levels. This progression is more evident at the SG but is still measurable in the SS. This enlargement of the cells during epidermal maturation may be the result

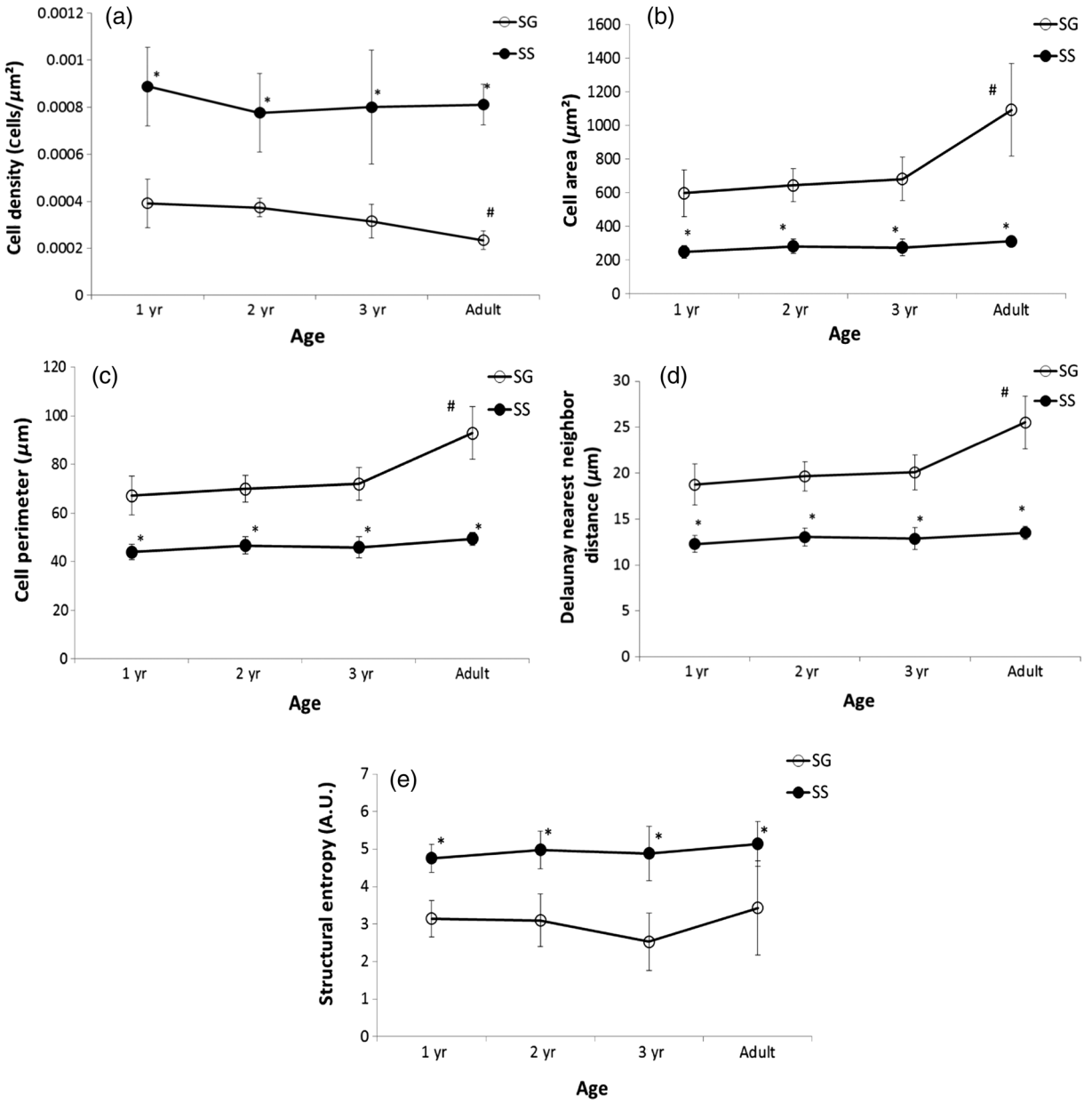

Fig. 2 Epidermal geometrical and topological parameters define the structure of the SS and the SG, and characterize the dynamics of these structures during skin maturation: (a) cell density, (b) cell projected area, (c) cell perimeter, (d) average Delaunay nearest-neighbor distance, and (e) structural entropy. Data are shown as mean $\pm$ one standard deviation; * indicates that the SS value is significantly different from the SG value; # indicates the one-year-old group value is significantly different from the adult group value.

of a gradual reduction in cell turnover rate with a concomitant thickening of the epidermal layers:[5] lower turnover rate and thicker layers result in longer residence time of the keratinocytes in the epidermis and, therefore, more time to mature and increase their projected area.[21] While geometrical parameters change with age, structural entropy appears to be preserved during the maturation processes of infant epidermal structure. Since our focus has been so far on healthy skin, it is tempting to hypothesize that this parameter may be altered in certain disease cases, particularly in hyper-proliferative disorders. Future work will shed more light into this hypothesis.

In a recent publication,[15] the authors analyze the dynamics of a cellular interaction network by using game theory. More specifically, they focused on the comparison between healthy and cancerous epithelial tissues. Cancer cells adopt a cheating behavior, following the prisoner's dilemma principle, leading to an abnormal intense proliferative state, and hence taking advantage of space expansion over the healthy tissue. This leads to a higher proportion of cells with few nearest neighbors (more positive skewness) as well as a small number of cells with an unusually high number of nearest neighbors (>8, defector distribution, red bars in Fig. 3).

The epidermis is a highly proliferative tissue as well, although cell division happens only at the basal layer. It is interesting to observe in this study that both for infant and adult skin, the probability of distribution of the number of nearest neighbors closely follows the cooperators model (blue bars in Fig. 3) with a maximum at 6. This type of network architecture is

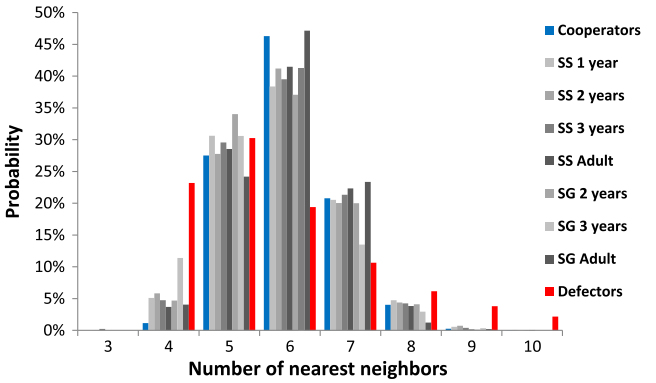

Fig. 3 The probability distribution of the number of nearest neighbors per cell for the SS and the SG, and for all age groups tested closely follows the cooperator model (blue bar) as opposed to the defector model (red bar). Model data are from Ref. 15.

typical of a cooperative behavior characteristic of healthy epithelial tissues, as opposed to the competitive defector behavior of tumor tissues. This result is in general agreement with the observed distribution in other healthy tissues for various organisms across different taxa.[15,22] Our conclusions, however, should be taken with prudence given the relatively low number of samples used in this study.

We have shown that geometrical and topological analysis of cell organization in RCM images can be used to quantify differences between two epidermal layers and between infant and adult skin. However, when having to analyze a large number of images, it can be tedious to manually mark the cell centers and analyze each image separately. Therefore, the possibility of automatic analysis using segmentation algorithms could provide a considerable advantage.

Using the proposed topological analysis on confocal images representing different skin conditions (healthy, atopic dermatitis, psoriasis, etc.) could provide new insights and markers for diagnosing and monitoring the efficacy of treatments.

Acknowledgments

The authors would like to thank Dr. Attila Csikász-Nagy for the nearest-neighbor frequency data of the cooperator and defector schemes. This work was fully funded by a research grant from Johnson & Johnson Santé Beauté France. G. N. S. and J. B. are employees of this company.

References

1. P. Corcuff and J. L. Lévêque, "*In vivo* vision of the human skin with the tandem scanning microscope," *Dermatology* **186**(1), 50–54 (1993).
2. S. González and Y. Gilaberte-Calzada, "In vivo reflectance-mode confocal microscopy in clinical dermatology and cosmetology," *Int. J. Cosmet. Sci.* **30**(1), 1–17 (2008).
3. M. Ulrich, S. Lange-Asschenfeldt, and S. Gonzalez, "Clinical applicability of *in vivo* reflectance confocal microscopy in dermatology," *G. Ital. Dermatol. Venereol.* **147**(2), 171–178 (2012).
4. M. Rajadhyaksha et al., "*In vivo* confocal scanning laser microscopy of human skin II: advances in instrumentation and comparison with histology," *J. Invest. Dermatol.* **113**(3), 293–303 (1999).
5. G. N. Stamatas et al., "Infant skin microstructure assessed *in vivo* differs from adult skin in organization and at the cellular level," *Pediatr. Dermatol.* **27**(2), 125–131 (2010).
6. G. Pellacani et al., "Reflectance confocal microscopy as a second-level examination in skin oncology improves diagnostic accuracy and saves unnecessary excisions: a longitudinal prospective study," *Br. J. Dermatol.* **171**(5), 1044–1051 (2014).
7. D. Gareau, "Automated identification of epidermal keratinocytes in reflectance confocal microscopy," *J. Biomed. Opt.* **16**(3), 030502 (2011).
8. J. Nikolovski et al., "Barrier function and water-holding and transport properties of infant stratum corneum are different from adult and continue to develop through the first year of life," *J. Invest. Dermatol.* **128**(7), 1728–1736 (2008).
9. G. N. Stamatas et al., "Infant skin physiology and development during the first years of life: a review of recent findings based on *in vivo* studies," *Int. J. Cosmet. Sci.* **33**(1), 17–24 (2011).
10. Y. B. Chiou and U. Blume-Peytavi, "Stratum corneum maturation. A review of neonatal skin function," *Skin Pharmacol. Physiol.* **17**(2), 57–66 (2004).
11. G. N. Stamatas, A. P. Morello, and D. A. Mays, "Early inflammatory processes in the skin," *CMM* **13**(8), 1250–1269 (2013).
12. G. Stamatas, "The structural and functional development of skin during the first year of life: investigations using non-invasive methods," in *Textbook of Aging Skin*, M. A. Farage, K. W. Miller, and H. I. Maibach, Eds., pp. 715–724, Springer, Berlin, Heidelberg (2010).
13. R. Marcelpoil and Y. Usson, "Methods for the study of cellular sociology: Voronoi diagrams and parametrization of the spatial relationships," *J. Theor. Biol.* **154**(3), 359–369 (1992).
14. M. Guillaud, C. Clem, and C. MacAulay, "An in silico platform for the study of epithelial pre-invasive neoplastic development," *Biosystems* **102**(1), 22–31 (2010).
15. A. Csikász-Nagy et al., "Cooperation and competition in the dynamics of tissue architecture during homeostasis and tumorigenesis," *Semin. Cancer Biol.* **23**(4), 293–298 (2013).
16. M. C. Gibson et al., "The emergence of geometric order in proliferating metazoan epithelia," *Nature* **442**(7106), 1038–1041 (2006).
17. T. Lecuit and P.-F. Lenne, "Cell surface mechanics and the control of cell shape, tissue patterns and morphogenesis," *Nat. Rev. Mol. Cell Biol.* **8**(8), 633–644 (2007).
18. A. Poupon, "Voronoi and Voronoi-related tessellations in studies of protein structure and interaction," *Curr. Opin. Struct. Biol.* **14**(2), 233–241 (2004).
19. R. Kamalov et al., "A Java application for tissue section image analysis," *Comput. Methods Progr. Biomed.* **77**(2), 99–113 (2005).
20. K. Kayser, G. Kayser, and K. Metze, "The concept of structural entropy in tissue-based diagnosis," *Anal. Quant. Cytol. Histol.* **29**(5), 296–308 (2007).
21. N. Kashibuchi et al., "Three-dimensional analyses of individual corneocytes with atomic force microscope: morphological changes related to age, location and to the pathologic skin conditions," *Skin Res. Technol.* **8**(4), 203–211 (2002).
22. B. Dubertret and N. Rivier, "The renewal of the epidermis: a topological mechanism," *Biophys. J.* **73**(1), 38–44 (1997).